

The underlying direction of the heliospheric magnetic field through the Ulysses first orbit

R. J. Forsyth and A. Balogh

The Blackett Laboratory, Imperial College, London, UK

E. J. Smith

Jet Propulsion Laboratory, Pasadena, CA

Abstract. Between February 1992 and April 1998, the Ulysses spacecraft carried out the first survey of how the properties of the solar wind and heliospheric magnetic field vary with latitude during the declining and minimum phases of the solar cycle. In this paper we report on how the underlying direction of the heliospheric magnetic field varied through the various phases of the Ulysses first solar orbit. To a first approximation both the azimuth angle of the magnetic field with respect to the radial direction and the meridional (north-south) angle agree with the predictions of the simple Parker spiral model. However there are a number of notable deviations. For example, at high southerly latitudes the most probable azimuth angle was found to be $\sim 24^\circ$ more tightly wound than expected, although the mean angle was less tightly wound than expected. In contrast, at high northerly latitudes, the most probable azimuth angle agreed with the Parker prediction, but the meridional angle showed a notably double peaked distribution. We discuss possible interpretations of these and other results in the context of recent ideas on the large scale behaviour of the heliospheric magnetic field. No evidence of a heliolongitude dependence of the underlying field, predicted by one model, is found. It is suggested that the presence of large scale Alfvén waves in the high latitude heliosphere may lead to double peak distributions of the magnetic field angles, consistent with evidence that longer time averaging removes some of the unexpected features noted in the results. Our analysis does not rule out that systematic deviations due to field line footpoint motions could be present but suggests that their amplitude may be too low to be reliably detected in in-situ heliospheric magnetic field data.

Introduction

The Ulysses spacecraft was launched in October 1990 equipped with a suite of instruments designed to provide a three dimensional characterisation of the heliosphere [e.g. *Marsden et al.*, 1996]. The unique polar orbit of the spacecraft around the Sun was established by a gravitational swing-by of Jupiter in February 1992. Beginning from this latitude of 6°S , the spacecraft reached maximum latitudes of 80.2° in both the southern and northern hemispheres in September 1994 and July 1995 respectively. The first ~ 6 year orbit of the Sun was completed when Ulysses again reached 6°S in April 1998. In this paper we will examine how the underlying direction of the heliospheric magnetic field varies with distance from the Sun and with heliographic latitude throughout this first full Ulysses orbit during the declining and minimum phases of the solar cycle.

The heliospheric magnetic field represents the outward extension of the Sun's magnetic field being carried out into interplanetary space frozen-in to the solar wind. Since the footpoints of the magnetic field lines are to a first approximation fixed in the solar photosphere, and if a radially outflowing solar wind with speed independent of both radial and latitudinal position is assumed, the combination of the Sun's rotation and the outflowing solar wind leads to the magnetic field lines being twisted up into an Archimedean spiral in the solar equatorial plane. This simple result was predicted by *Parker* [1958] and received observational confirmation when early spacecraft measurements of the interplanetary magnetic field

[*Ness and Wilcox*, 1964] showed that the field lines were orientated at $\sim 45^\circ$ with respect to the radial direction, and lay approximately in the equatorial plane, in the vicinity of the Earth. In this picture, at any chosen latitude away from the equatorial plane the field lines can be viewed as wrapped around conical surfaces with half angle equal to the colatitude. Thus the angle between the field lines and the radial direction would be expected to decrease with increasing latitude, until a field line originating from the Sun's rotational pole should be purely radial. In equation form, the azimuth angle ϕ_P that the tangent to an ideal Parker model magnetic field line makes with the radial direction is given by

$$\tan \phi_P = \frac{v_\phi - \Omega r \cos \delta}{v_r} \quad (1)$$

where Ω is the solar rotation rate, v_r and v_ϕ are the radial and azimuthal components of the solar wind velocity, and r and δ are the heliocentric distance and heliographic latitude describing the position of the observing spacecraft. The derivation of this equation does not require the assumption that the solar wind speed is independent of radial and latitudinal position and thus predicts ϕ_P given the locally measured solar wind speed. In practice, v_ϕ is small enough to be ignored in most analyses. In investigating the magnetic field direction we use Parker's model to organise our data and study deviations of the magnetic field direction from the expected azimuth angle ϕ_P and expected meridional angle of 0° [e.g. *Smith*, 1997 (appendix)].

A number of spacecraft have explored the heliosphere near the ecliptic plane and have shown that Parker's spiral model holds to a first approximation over a wide range of heliocentric distances – between 1 and ~8 AU from Pioneer data [Thomas and Smith, 1980] and from Voyager data [Burlaga *et al.*, 1982], in the more distant heliosphere [Burlaga and Ness, 1993], and within 1 AU from Helios data [e.g. Bruno and Bavassano, 1997].

Ulysses is the only spacecraft to have explored the heliosphere over a wide range of latitudes away from the ecliptic plane. Figure 1 shows the expected variation of $-\phi_p$ round the complete Ulysses first orbit. This angle is commonly referred to as the spiral angle and is a measure of the angle between an antisunward directed field line and the radial direction. It has been calculated using equation 1 taking account of the position of Ulysses and the solar wind speed measured by the solar wind plasma instrument [Bame *et al.*, 1992]. The solar rotation rate, Ω , used is that corresponding to a period of 25.38 days, the value at the equator. The dominant effect is the changing latitude of the spacecraft leading to a spiral angle of approximately 10° at the highest latitudes compared to near 80° in the equatorial regions at 5.4 AU. The effect of distance from the Sun can be seen by comparing the 50° angle as Ulysses crossed the equatorial plane at 1.3 AU during the fast latitude scan in 1995 with the 80° angle at 5.4 AU. The effect of changing solar wind speed is seen in the fine detailed variations superimposed on the main trend – the spiral is less tightly wound when the wind speed is faster. The influence of the alternating fast and slow solar wind streams encountered by Ulysses in 1992/93 and 1996/97 can be clearly seen [e.g. McComas *et al.*, 2000].

A number of results on the underlying magnetic field direction during the Ulysses first orbit have already been reported [Forsyth *et al.*, 1995; 1996a; 1996b], obtained by analysing distributions of the direction calculated from hourly averaged magnetic field data. As Ulysses travelled southwards for the first time in 1993 and 1994 under solar activity conditions declining towards minimum, the spacecraft eventually became continuously immersed in fast solar wind from the Sun's southern polar coronal hole [Phillips *et al.*, 1994]. In this region it was found [Forsyth *et al.*, 1996a] that the most probable value of the azimuth angle describing the magnetic field direction agreed well with the prediction of the simple spiral model described above. However the distribution of the azimuth angle was significantly biased towards field directions less tightly wound than the prediction. Forsyth *et al.* [1996a] concluded that the most likely reason for this behaviour was the presence of large amplitude Alfvén waves with periods of many hours in the high speed solar wind [Smith *et al.*, 1995; 1997b]. As Ulysses continued through the highest southerly latitudes, the most probable value of the azimuth angle distribution moved to become of the order of 24° more tightly wound than expected in a distribution accumulated at latitudes greater than 60° , even though the bias towards less tightly wound angles continued [Forsyth *et al.*, 1995]. However, this result was not reproduced in the same latitude range in the northern hemisphere, where the most probable value of the azimuth angle again agreed with the Parker model [Forsyth *et al.*, 1996b]. Smith *et al.* [1997a] point out a very short interval at high northern latitudes where the azimuth angle became approximately 0° which they suggest is evidence of

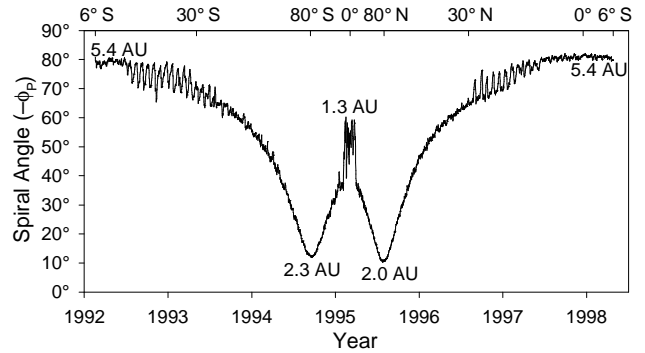


Figure 1. The expected variation of the spiral angle, $-\phi_p$, around the complete Ulysses first orbit of the Sun, calculated using the position of Ulysses and the measured solar wind speed. The latitude of the spacecraft is shown along the top axis and the heliocentric distance is labelled at key points.

magnetic field lines connected to the Sun's rotational pole. A further recent report points out a high degree of underwinding in corotating rarefaction regions observed by Ulysses between approximately $30 - 20^\circ$ N [Smith *et al.*, 2000]. Previously published results on the meridional angle, only from the southern polar pass prior to the present work, indicate agreement of the most probable angle with the Parker prediction of 0° [Forsyth *et al.*, 1995; 1996a]. Again broad distributions were found, most likely due to the presence of Alfvén waves.

Fisk [1996] has proposed a more sophisticated model of the heliospheric magnetic field which takes account of the expected magnetic field line footpoint motion in the photosphere. This model was introduced with the aim of explaining why energetic particle enhancements associated with the reverse shocks of corotating interaction regions reached Ulysses at higher heliographic latitudes than those where the shocks were observed in-situ [e.g. Sanderson *et al.*, 1995; Roelof *et al.*, 1996]. The idea is that there should be a magnetic field connection to reverse shocks at lower latitudes than Ulysses at a distance further from the Sun. Whereas the Parker model assumes that field line footpoints corotate with the Sun at a rate independent of latitude, Fisk's model introduces two additional effects. The first is differential rotation – the fact that the photosphere is observed to rotate more slowly at higher latitudes. The second effect is that near solar minimum, magnetic field lines in the heliosphere mainly originate from the polar coronal holes. Coronal holes have been observed to rotate rigidly (i.e. at a rate independent of latitude) with the Sun to first approximation, and the polar holes are presumed to be centred on the Sun's magnetic poles rather than the rotational poles. The magnetic axis has a tilt with respect to the rotation axis which is solar cycle dependent, being close to 0° at solar minimum, and, for example, approximately 30° at the time of the Ulysses passage to high southerly latitudes. Among the consequences of these effects is to produce field lines in the heliosphere whose azimuth and meridional angles have a heliographic longitude dependence, and which in some locations provide the required connection between high and low heliographic latitudes between about 5 and 15 AU. Zurbuchen *et al.* [1997] present evidence which they suggest explains the Ulysses high latitude southern hemisphere magnetic field observations in terms of this model. It should be stressed that this model is only likely to produce predictable deviations from the Parker model given the quasi-stable (over

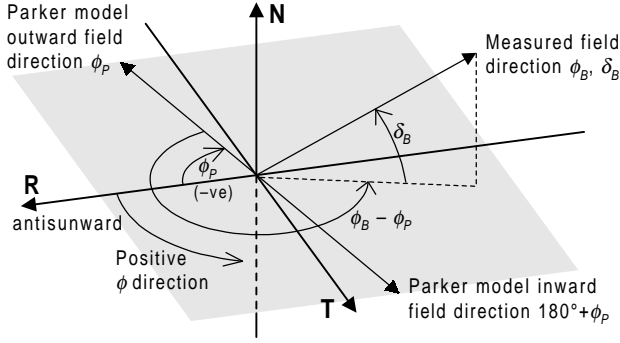


Figure 2. Definitions of the azimuth angle deviation and meridional angle deviation with respect to the RTN coordinate system. The example shown is for a sunward magnetic field vector.

many solar rotations) coronal magnetic field configuration applicable during the declining and minimum phases of the solar cycle.

The aim of this paper is to present the full set of magnetic field direction observations from the Ulysses first orbit. In particular the meridional angle distributions from the north polar pass and both the meridional and azimuthal angle distributions from the final phase of the orbit, returning from high northerly latitudes, have not yet been published. We then go on to discuss whether the observed departures from the simple Parker model can be explained in terms of the *Fisk* model or other possible causes.

Observations

We work in the spacecraft centred heliospheric RTN coordinate system where the R axis points in a direction radially outwards from the Sun and the RT plane is inclined to the equator at an angle equal to the heliographic latitude of the spacecraft. In this reference system a field line in agreement with the Parker model should lie in the RT plane at all latitudes. The coordinate system and the definitions of the azimuthal and meridional angle deviations are shown in Figure 2. The azimuth angle ϕ_B and meridional angle δ_B defining the magnetic field direction are calculated (see Appendix A) from hourly averaged magnetic field data measured by the magnetometer onboard Ulysses [Balogh *et al.*, 1992]. From these hourly values ϕ_B and δ_B we calculate their deviations from the direction predicted by the Parker model ($\phi_P, 0^\circ$) as $\phi_B - \phi_P$ and δ_B . Thus if the measured field directions agree with the predictions we should find $\phi_B - \phi_P = 0^\circ$ in regions of antisunward

directed field and $\phi_B - \phi_P = 180^\circ$ in regions of sunward directed field. Once the deviations from the Parker model, $\phi_B - \phi_P$ and δ_B , have been obtained, they are binned into histograms to allow us to study their distributions.

For the purposes of this survey of the complete first orbit we have divided the orbit into ten sub-intervals and obtained histograms for each of these. These sub-intervals have been chosen based on changes in the solar wind speed and magnetic field polarity round the Ulysses orbit. We use the terms slow scan and fast scan to identify the aphelion and perihelion phases of the orbit respectively. The intervals are 1) $6^\circ\text{S} - 30^\circ\text{S}$ beginning from after the Jupiter flyby in February 1992 as Ulysses began to travel southwards away from the ecliptic plane. Both magnetic field polarities were still present in the data and corotating interaction regions were dominant; 2) $30^\circ\text{S} - 60^\circ\text{S}$ where only inward polarity magnetic fields were detected; 3) $> 60^\circ\text{S}$, the highest southerly latitudes where unexpected changes in the azimuth angle were previously reported; 4) $60^\circ\text{S} - 23^\circ\text{S}$ during the fast latitude scan where only inward polarity fields and uniform fast solar wind were observed; 5) $23^\circ\text{S} - 20^\circ\text{N}$, the equatorial part of the fast latitude scan when both field polarities were present; 6) $20^\circ\text{N} - 60^\circ\text{N}$ during the fast latitude scan where only outward polarity fields were observed; 7) $> 60^\circ\text{N}$, the highest northern latitudes; 8) $60^\circ\text{N} - 30^\circ\text{N}$ during the slow latitude scan where only outward polarity fields and uniform fast solar wind were observed as Ulysses returned from high northern latitudes; 9) $30^\circ\text{N} - 7^\circ\text{N}$ where corotating interaction regions and both magnetic field polarities were once again observed; and finally 10) $7^\circ\text{N} - 7^\circ\text{S}$ where Ulysses traversed the equatorial regions at aphelion to close the first orbit. 7°S was chosen as the end point for this last region rather than 6°S so that a symmetrical range of latitudes about the equator was enclosed.

Figure 3 presents the azimuth angle distributions of $\phi_B - \phi_P$, using 10° wide bins, for these ten intervals. In addition Tables 1 and 2 provide information on some of the statistical properties of the distributions. In Table 1 the statistics are all calculated using only data lying within $\pm 90^\circ$ of the expected values of $\phi_B - \phi_P$. This is so that all the distributions can be directly compared to each other. Table 2, on the other hand, provides statistics calculated from the full range of data in the distributions where only a single field polarity is present. The horizontal axes on Figure 3 have been plotted running from -90° to 270° . Thus the distributions of outward polarity field lines appear in the left hand half of the figures centred on 0° while the distributions of inward polarity field lines appear in the right hand half of the figures centred on 180° . Histogram bins

Table 1. Statistics of Azimuthal Angle Distributions

Latitude Range	No. of obs.	Mean Values $^\circ$		Most Probable $^\circ$		% $< 0^\circ$	% $> 0^\circ$	% $< 180^\circ$	% $> 180^\circ$
$6^\circ\text{S} - 30^\circ\text{S}$	10520	-2.9 ± 0.6	184.6 ± 0.5	0 ± 5	182 ± 5	55%	45%	44%	56%
$30^\circ\text{S} - 60^\circ\text{S}$	8212		187.0 ± 0.4		181 ± 4			45%	55%
$> 60^\circ\text{S}$	5446		183.6 ± 0.6		158 ± 13			49%	51%
$60^\circ\text{S} - 23^\circ\text{S}$	1522		186.2 ± 0.8		182 ± 8			44%	56%
$23^\circ\text{S} - 20^\circ\text{N}$	1331	-4.1 ± 1.5	191.2 ± 1.4	-5 ± 12	181 ± 6	54%	46%	38%	62%
$20^\circ\text{N} - 60^\circ\text{N}$	1439		7.0 ± 0.9		2 ± 9	44%	56%		
$> 60^\circ\text{N}$	4176		5.2 ± 0.7		0 ± 5	46%	54%		
$60^\circ\text{N} - 30^\circ\text{N}$	6136		5.0 ± 0.5		-9 ± 5	48%	52%		
$30^\circ\text{N} - 7^\circ\text{N}$	8642	2.5 ± 0.5	(175.3 ± 1.3)	4 ± 9	(158 ± 10)	46%	54%	(58%)	(42%)
$7^\circ\text{N} - 7^\circ\text{S}$	6736	0.2 ± 0.5	180.2 ± 0.6	3 ± 10	184 ± 5	49%	51%	48%	52%

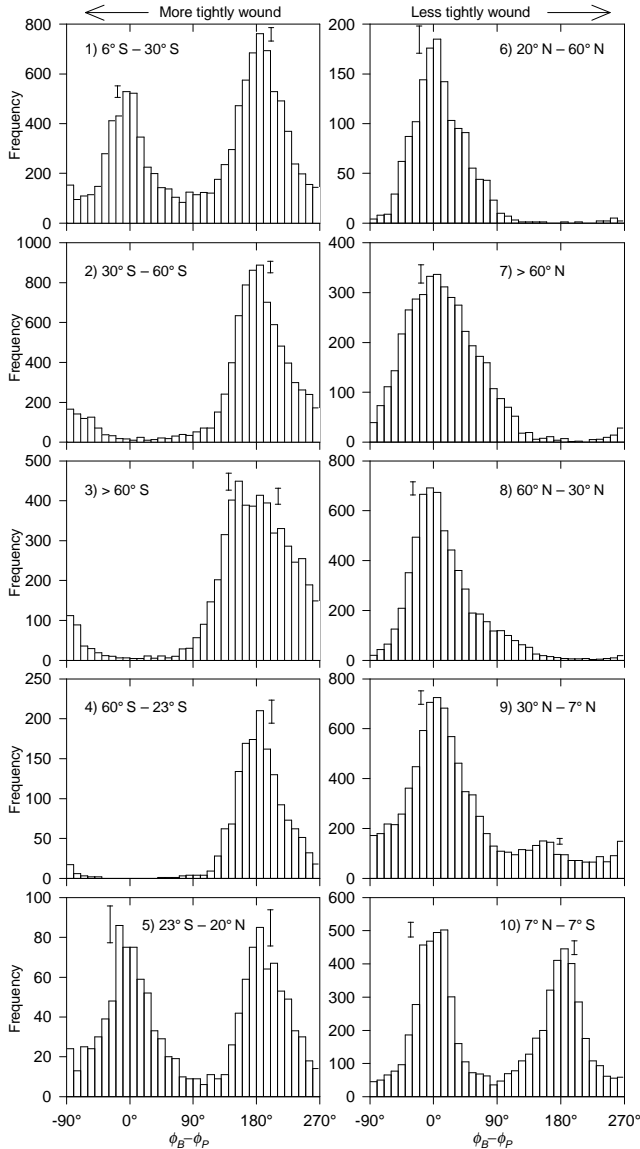


Figure 3. Histograms of the deviation in azimuth angle, $\phi_B - \phi_P$, from that predicted by the Parker model of the heliospheric magnetic field for the different sections of the Ulysses first orbit. The subdivisions of the orbit are described in the text. On this and subsequent figures, the error bars drawn next to each peak represent the statistical error in the height of the maximum bin.

to the left of the expected values indicate field lines more tightly wound than the Parker prediction while those to the right indicate less tightly wound field lines.

The absence of outward directed field lines in the unipolar region of the southern hemisphere can be clearly seen in panels 2, 3 and 4, and the absence of inward directed field lines in the northern hemisphere is obvious in panels 6, 7 and 8. This is consistent with the near solar minimum heliospheric magnetic field configuration. Note that in these regions it can be seen that the wings of the single distributions present extend more than $\pm 90^\circ$ from their central values. This behaviour and the reasons for it have recently been discussed in detail by *Balogh et al.* [1999]. It is interesting to note that in region 9, where inward polarity fields had returned, the percentage of

Table 2. Statistics of Full Width Distributions

Latitude Range	Mean $^\circ$	% < (18)0 $^\circ$	% > (18)0 $^\circ$
30 $^\circ$ S – 60 $^\circ$ S	193.6 \pm 0.6	42%	58%
> 60 $^\circ$ S	187.4 \pm 0.7	47%	53%
60 $^\circ$ S – 23 $^\circ$ S	187.4 \pm 0.9	44%	56%
20 $^\circ$ N – 60 $^\circ$ N	7.5 \pm 1.0	44%	56%
> 60 $^\circ$ N	10.2 \pm 0.8	44%	56%
60 $^\circ$ N – 30 $^\circ$ N	12.3 \pm 0.6	45%	55%

time for which they are present compared to the dominant outward polarity is very small. This is likely due to the fact that although the tilt of the heliospheric current sheet was small at this time, the presence of a warp in the current sheet at one localised longitude region led to the return of sector structure in the Ulysses data at higher latitudes than expected [*Forsyth et al.*, 1997].

Examining all the distributions in Figure 3, it is clear that the only distribution which has a most probable value significantly different from expected is that of interval 4) at high southerly latitudes greater than 60° . As previously reported this distribution has a most probable value approximately 24° more tightly wound than expected. Note that this distribution does appear to be double peaked, i.e. there are two populations of preferred angles, with a secondary peak close to the expected value of 180° . It may be within statistical chance that the histogram bin centred on 155° has a higher frequency compared to the one centred on 185° . This behaviour is not reproduced in the distribution accumulated at the equivalent latitudes in the northern hemisphere. Indeed, in all the new data presented here, as Ulysses traversed the northern hemisphere and returned to the ecliptic regions at 5.4 AU at aphelion, the most probable values of the distributions are clearly in line with the predictions of the Parker model to a good first approximation. The only further exception is for the minority southern hemisphere polarity distribution on the right hand half of panel 9 where the small number of observations don't give good statistics. A qualitative difference for the two high latitude periods in panels 3) and 7) is that the distributions are less sharply peaked and broader than the others presented.

The further feature of the distributions that is now confirmed around the full orbit is that in all the periods where Ulysses is sampling a single field polarity and uniform high speed solar wind, the mean values of the distributions are strongly biased in an underwound direction, despite the most probable values not showing bias in most cases. This behaviour is independent of whether Ulysses is in the southern or northern hemisphere of the heliosphere or of which field polarity is being sampled. The statistical reason for this bias in the mean values is that the distributions are highly asymmetric. In all the relevant cases, panels 2, 3, 4 and 6, 7, 8, the percentage of observations greater than 0 or 180° , i.e. underwound from expected, is higher than the percentage less than 0 or 180° . This is clearly shown in the rightmost two columns of Table 2. Thus we again emphasise the danger of reporting mean values of the winding angle of the heliospheric magnetic field without carefully examining the distributions from which they are obtained. As already stated, it is likely that this effect is a consequence of the presence of Alfvén waves in the fast solar wind and is perhaps due to the fact that they are

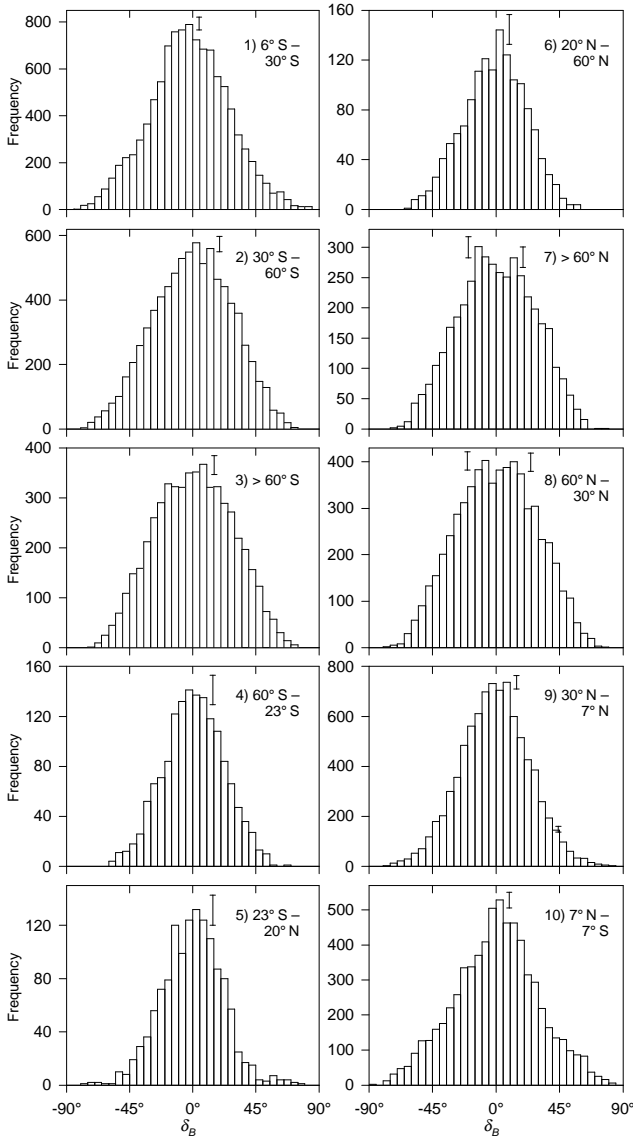


Figure 4. Histograms of the deviation in meridional angle, δ_B , from that predicted by the Parker model of the heliospheric magnetic field for the different sections of the Ulysses first orbit.

propagating radially rather than along the field. It may be that a simple simulation could be used to confirm this hypothesis.

Finally, considering panels 1, 5 and 10 where both polarity peaks are present, we see that the enclosed angle between the northern and southern hemisphere mean values is not exactly 180° in two out of the three cases, the exception being panel 10. This behaviour is consistent with previous near-ecliptic results where field lines north of the heliospheric current sheet have been found to be more tightly wound than those south of the heliospheric current sheet [e.g. *Smith and Bieber, 1993*]. In panel 10 neither peak has a mean value significantly different from ϕ_p .

Turning now to the meridional angle distributions, these are reproduced in Figure 4 using a 5° bin width, with accompanying statistical data in Table 3. Here all the distributions are approximately symmetrical and all, apart from panel 1, have mean values which agree with the expected value of $\delta_B = 0^\circ$. Apart from in panel 7, the most probable values are in

Table 3. Statistics of Meridional Angle Distributions

Lat. Range	Mean $^\circ$	M. Prob. $^\circ$	% $< 0^\circ$	% $> 0^\circ$	St. Dev. $^\circ$
$6^\circ\text{S} - 30^\circ\text{S}$	-2.1 ± 0.3	-7 ± 4	53%	47%	27.7
$30^\circ\text{S} - 60^\circ\text{S}$	0.1 ± 0.3	1 ± 3	49%	51%	27.7
$> 60^\circ\text{S}$	0.9 ± 0.4	5 ± 2	49%	51%	27.5
$60^\circ\text{S} - 23^\circ\text{S}$	0.7 ± 0.6	-1 ± 5	49%	51%	21.4
$23^\circ\text{S} - 20^\circ\text{N}$	-0.4 ± 0.6	4 ± 3	49%	51%	21.5
$20^\circ\text{N} - 60^\circ\text{N}$	-1.0 ± 0.6	3 ± 2	50%	50%	21.9
$> 60^\circ\text{N}$	0.4 ± 0.4	-8 ± 6	50%	50%	26.8
$60^\circ\text{N} - 30^\circ\text{N}$	0.6 ± 0.4	3 ± 9	49%	51%	27.8
$30^\circ\text{N} - 7^\circ\text{N}$	-0.8 ± 0.3	1 ± 6	51%	49%	24.1
$7^\circ\text{N} - 7^\circ\text{S}$	0.2 ± 0.4	1 ± 2	48%	52%	29.4

agreement with the mean values, consistent with the symmetrical distributions. A new observation which emerges in intervals 7) and 8), that is at high northern latitudes greater than 60°N and for latitudes descending back to 30°N after the north polar pass, is that here there appears to be a double peak in the distribution $\sim 10\text{-}15^\circ$ either side of the centre with a dip in between the two peaks, all symmetrical about the centre. In interval 7) the most probable value is associated with the peak on the negative side of the expected value, while in interval 8) neither peak is more prominent than the other. Such behaviour is not apparent in the equivalent distributions accumulated over the same latitude ranges in the southern hemisphere.

A notable feature of panels 4, 5 and 6 is that these distributions appear narrower than the others. Since the distributions are approximately symmetrical, we have attempted to quantify this by listing their standard deviations in Table 3. It can be seen that distributions 4, 5 and 6 have standard deviations of the order of 21° while the majority of the others tend to be around 27° . The distinguishing features of these distributions are that they are accumulated at smaller heliocentric distances than the others and that they are accumulated from fewer observations than the others. As would be expected, histograms constructed from a similarly small number of observations in other latitude ranges, were found to have standard deviations consistent with the data in Table 3 for the interval in which they were obtained. This leaves a distance effect as the most likely explanation. We note that this interpretation is qualitatively consistent with the results of *Burlaga and Ness [1997]* who compared distributions of δ_B obtained at 1 AU with those obtained by the Voyager spacecraft between 40 and 62 AU. Magnetic field fluctuation studies have indicated that the field component amplitude for timescales appropriate to hourly averages decreases with distance from the Sun [e.g. *Horbury and Balogh, 2001*] opposite to the trend we note here. However, the δ_B distribution widths will depend critically on how the field magnitude falls off with distance in comparison.

Discussion and Further Analysis

Heliolongitude Effects

We first turn our attention to the highest latitude southern and northern hemisphere distributions, in particular the overwound most probable azimuth angle in Figure 3, panel 3, and the double peaked meridional angle in Figure 4, panel 7. A possible interpretation of these results is that the additional peaks in the distributions are related to the heliolongitude

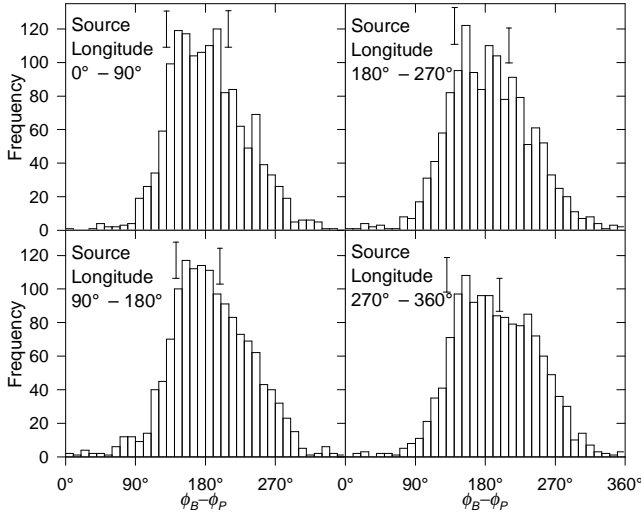


Figure 5. Azimuth angle distributions accumulated over nine solar rotations while Ulysses was at high southerly latitudes. The four distributions are separated depending on the source heliolongitude obtained by mapping back the solar wind reaching Ulysses.

dependence of the field direction predicted by the model of *Fisk* [1996], but absent in the simple Parker model. This heliolongitude effect should lead to field lines overwound with respect to the Parker model for half a solar rotation, and field lines underwound from expected for the other half.

To test this scenario, we have analysed firstly the southern hemisphere azimuth angle distribution by subdividing it based on the heliolongitude (specifically, the Carrington longitude) of the footpoints of the magnetic field lines. The footpoints were determined by mapping back the solar wind arriving at Ulysses under the assumption that it had travelled at constant speed out from the Sun at the same speed as measured at Ulysses. Then histograms were constructed separately for those hourly measurements with footpoints in the 36 overlapping longitude ranges $0^\circ\text{--}90^\circ$, $10^\circ\text{--}100^\circ$, $20^\circ\text{--}110^\circ$, ..., $350^\circ\text{--}80^\circ$. To ensure no bias due to only including part of a solar rotation period, the length of time analysed was adjusted so that it covered exactly nine solar rotations. The revised time period used was days 099–333 inclusive of 1994 when Ulysses traversed the latitude range from 59°S to 80.2°S and back to 60°S . This includes the subset of the data analysed by *Zurbuchen et al.* [1997] discussed in more detail in the next section. The use of a ballistic or constant speed mapping back technique is often a gross approximation because of interactions that take place between solar wind streams travelling at different speeds in the course of their journey out from the Sun. However, because Ulysses sampled relatively constant solar wind speed at these high latitudes, the calculated source longitudes are less likely to be affected. This is supported by the finding that the number of observations in each of the subdivisions is approximately equal.

The results of this analysis are illustrated in Figure 5 using a selection of four histograms from the set of 36. Although the profile of the distributions is noisier due to the reduced number of observations in each histogram, in all 36 cases there is a well defined local maximum in the distributions near $\phi_B - \phi_P = 155^\circ$. In 25 out of the 36 cases a clear subsidiary local maximum is present near $\phi_B - \phi_P = 190^\circ$. Those distribu-

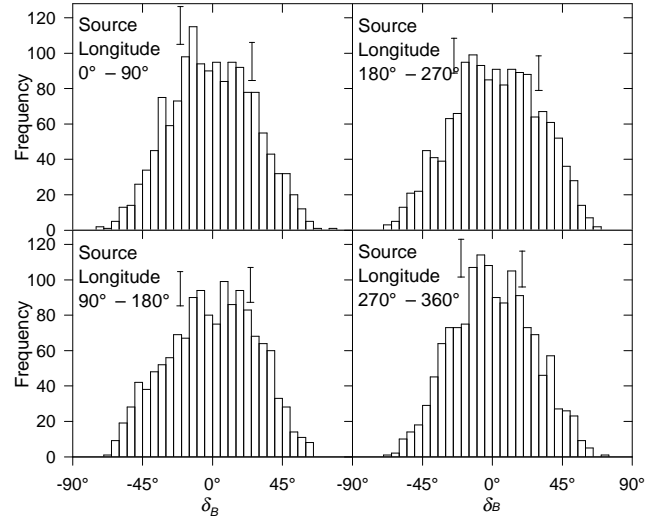


Figure 6. As for Figure 5, but showing meridional angle distributions accumulated over nine solar rotations while Ulysses was at high northerly latitudes.

tions from which this subsidiary maximum is absent are confined to two longitude ranges which include the lower two panels of Figure 5. These results suggest that the overwound most probable angle seen in the southern hemisphere high latitude distributions is not limited to specific source heliolongitudes.

Figure 6 shows four selected histograms from a similar analysis carried out for the meridional angle in the high latitude northern hemisphere observations. Again a time interval corresponding to nine solar rotations was used for the analysis. However, because the major axis of the Ulysses orbit is tilted slightly (6°) with respect to the equator, Ulysses traversed a greater range of latitudes over this time period than was the case in the southern hemisphere analysis presented above. The time period used was day 148 of 1995 to day 026 of 1996 inclusive during which time Ulysses travelled from 59°N through 80.2°N and back down to 50°N . This period includes data from both panels 7 and 8 of Figure 4, both of which show evidence of a double peaked distribution.

Again the distributions in Figure 6 are noisier than their combined parent distribution. A clear double peak is present in 23 out of the 36 distributions. Those in Figure 6 for $0^\circ\text{--}90^\circ$ and $180^\circ\text{--}270^\circ$ source longitude are examples of where at least one of the peaks cannot be distinguished clearly. In all 36 cases, however, the local maximum near $\delta_B = -10^\circ$ (equatorward from expected) was clearly discernible. The distributions for which the local maximum in the vicinity of $\delta_B = +10^\circ$ was less clear were again confined to two longitude ranges. However in all these cases, due to the variability of the distributions, it was not possible to conclusively say that it was absent. Thus it is also hard to argue that the double-peaked nature of the high latitude northern hemisphere distribution is confined to any particular range of heliolongitudes.

In the course of the above analyses we also subdivided the southern hemisphere high latitude meridional angle distribution and the northern hemisphere high latitude azimuth angle distribution, although neither of these had shown unexpected behaviour. In both cases a small number of the subdivisions showed evidence of a double peak even though the effect had been washed out in the parent distribution.

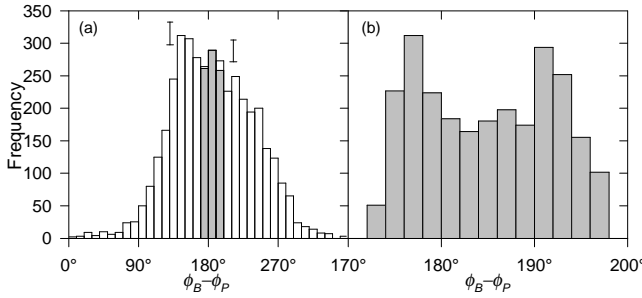


Figure 7. (a) Histogram of azimuthal angle deviations from the Parker model for latitudes $>66^\circ\text{S}$. Superimposed is the distribution predicted by applying the model of *Zurbuchen et al.* [1997] plotted using an arbitrary frequency scale. (b) An expanded version of the model predicted distribution using 2° wide bins to show the detail, also with an arbitrary frequency scale.

Direct Comparison With the *Fisk* Model

Zurbuchen et al. [1997] has published a comparison of the Ulysses high latitude southern hemisphere results with the predictions of the model of *Fisk* [1996] described in the introduction and the previous section. The equations and solar parameters presented in *Zurbuchen et al.* [1997] make it possible to assess the possible effects on our $\phi_B - \phi_P$ and δ_B histograms for the same subset of the data. This is the aim of this section. The equations for the field components in spherical polar coordinates are given by *Zurbuchen et al.* as:

$$B_r = B_0 (r_0/r)^2 \quad (2)$$

$$B_\theta = \frac{B_0 r_0^2}{Vr} \omega \sin \beta \sin(\phi + \Omega r/V - \phi_0) \quad (3)$$

$$B_\phi = \frac{B_0 r_0^2}{Vr} \left[\omega (\cos \beta \sin \theta + \sin \beta \cos \theta \cos(\phi + \Omega r/V - \phi_0)) - \Omega \sin \theta \right] \quad (4)$$

where B_0 is the magnetic field strength at the source surface located at heliocentric distance $r = r_0$, V is the solar wind speed, Ω is the solar rotation rate, ω is the differential rotation rate of the magnetic field line footpoints, β is the polar angle at which a field line originating from the rotational pole crosses the source surface and is related to the angle between the solar magnetic dipole axis and the rotation axis, ϕ_0 is the heliolongitude of the plane defined by the rotation and magnetic axes, and r , θ , ϕ are the heliocentric distance, colatitude and heliolongitude of the spacecraft. These can be adapted for use in *RTN* coordinates by taking $B_R = B_r$, $B_T = B_\theta$ and $B_N = -B_\phi$. In addition we replace the $\sin \theta$ terms with $\cos \delta$ where δ is the heliographic latitude of Ulysses. ϕ_B and δ_B can then be calculated in the usual way (Appendix A, equations A1). *Zurbuchen et al.* [1997] applied these equations in particular to data obtained when Ulysses was at latitudes higher than 66°S , pointing out that the boundaries of the southern polar coronal hole were particularly stable during this time, using $\omega = 0.068$ radians/day, $\beta = 30^\circ$, and $\phi_0 = 100^\circ$. For calculating the angles B_θ and r_0 are not required.

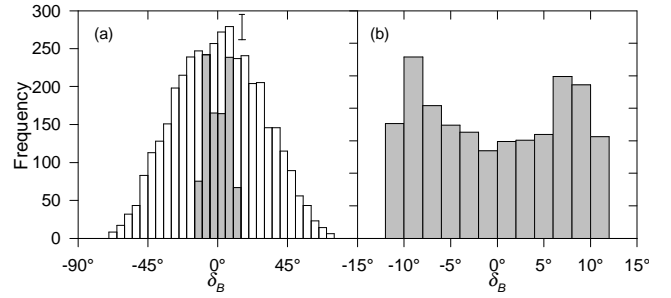


Figure 8. As for Figure 7, but in this case showing observed and model predicted histograms for the meridional angle for latitudes $>66^\circ\text{S}$.

The first panel (a) of Figure 7 shows the azimuthal angle histogram obtained from Ulysses data for the same latitude range as analysed by *Zurbuchen et al.* [1997]. The most probable angle in the vicinity of 150° is still clear in this reduced latitude range. Over-plotted in grey is the model predicted distribution. It is much narrower because the distribution has not been broadened by the Alfvén waves present in the real data so its height has been scaled to allow easier comparison with the data. On this scale the model appears to predict a narrow spread about the Parker direction. Panel (b) shows an expanded version of the model distribution using 2° wide bins to bring out the detail, again plotted with an arbitrary frequency scale. It is clearly a double peaked distribution but with a greater bias of points on the underwind side of the Parker prediction. It is unlikely that, even with broadening of this distribution by Alfvén waves, the peak in the model distribution at $\sim 177^\circ$ could be shifted enough to be responsible for the overwind most probable angle in the measured distributions.

Figure 8 shows the equivalent results for the meridional angle distributions. In this case the distribution predicted by the model, over-plotted on panel (a), clearly shows a double peak. This is shown in more detail in panel (b). In this region the observed distribution was not double peaked. However, a number of the other observed meridional angle distributions were double peaked, particularly in the northern hemisphere. Comparing the model and the observed distributions in panel (a), it is not ruled out that if the model distribution was broadened by Alfvén waves, a result similar to the observations could be obtained.

Examination of the time series resulting from the application of equations (2) to (4) reveals a dominant sinusoidal pattern at approximately the solar rotation period. It is clear that the double peaked distributions arising from the model are a result of this behaviour, being due to the greater number of points near the maxima and minima of the sine wave. If we apply a heliolongitude analysis (such as in Figure 6) to the model prediction for the meridional angle we find that only one of the peaks dominates in any one 90° heliolongitude range. We have tested whether a heliolongitude analysis of the southern hemisphere meridional angle follows a similar behaviour by overlaying model and data distributions in the 90° ranges. No evidence of a consistent variation in phase was found, in agreement with the result of Figure 6 that there is no clear heliolongitude dependence in the observations.

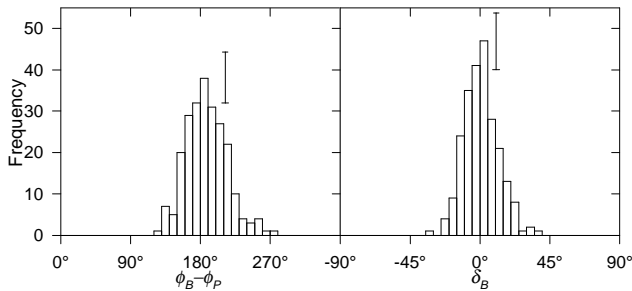


Figure 9. Histograms of the azimuthal and meridional angle deviations from the Parker model direction at high southerly latitudes, calculated from daily averages of the magnetic field components.

Results of Longer Time-Averaging

If, as has been proposed [e.g. Forsyth *et al.*, 1996a], the unexpected field directions observed in the high heliolatitude Ulysses data are due to the presence of the large amplitude Alfvén waves, then it is reasonable to expect that the effects would disappear if we extend the averaging period to something longer than the hourly averages we have used in our standard analysis. As the Alfvén waves have periods of the order of hours upwards [Smith *et al.*, 1995], it is not surprising that they have a major influence on our distributions. Indeed, we might ask whether the Alfvén waves could be responsible for the double-peaked distributions in our data in a similar way to that in which the sine wave produced a double peak in the model distributions of the previous section.

We have repeated our analysis of the high latitude southern and northern hemisphere data using the same nine-solar-rotation data set as previously, except that this time we used daily averages of the magnetic field data to calculate the angles, rather than hourly averages. The results are shown in Figures 9 and 10 for the southern and northern hemispheres respectively. In each case the left hand panel shows the azimuthal angle and the right hand panel the meridional angle histogram. Beginning with the left hand panel of Figure 9, it is clear that on this daily average timescale there is no longer any evidence of an overwound most probable angle, supporting our hypothesis that the Alfvén waves may be responsible.

However, bearing in mind the problem of asymmetric distributions of the azimuthal angle, some further discussion is required. If we had simply taken daily averages of the hourly azimuthal angles calculated earlier, we would clearly have obtained a result biased more towards the Parker model because the asymmetry of the distributions would naturally pull the mean in that direction (i.e. towards more positive or underwound angles). Inspecting distributions of the magnetic field components shows that they too are often asymmetric suggesting that mean values could easily depend on the time averaging of the data set one started from. We have been consistent in this paper in always calculating our hourly or daily averages from the full time resolution data set as described in Appendix A.

Turning our attention to the meridional angle plot on the right of Figure 9, we also find a narrower distribution than that obtained from hourly averages and consistent with $\delta_B = 0$ as were the hourly averages in this region. Appendix A includes an important caveat on the calculation of δ_B which can

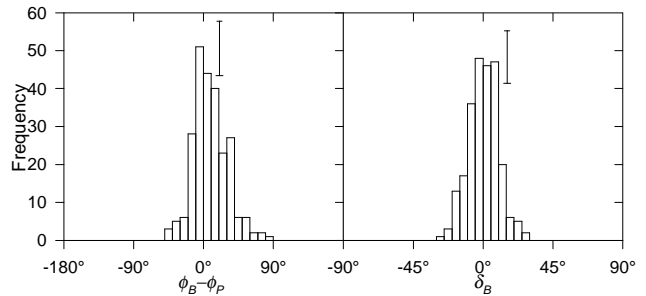


Figure 10. Histograms of the azimuthal and meridional angle deviations from the Parker model direction at high northerly latitudes, calculated from daily averages of the magnetic field components.

lead to major errors particularly in the case of daily averages.

Both histograms in Figure 10 for the northern hemisphere data also show most probable angles within one histogram bin width of the Parker model predictions. This is the region in which the meridional angle showed a double-peaked distribution when using hourly averaged data. This double peak is not apparent using the daily averaged data although we note that the peak of the distribution is three bins wide compared to the others in Figures 9 and 10 which are one bin wide. Thus we can say in general that deviations of the magnitude observed in the hourly average data are absent from the daily averaged data. This supports an interpretation that variability between these two timescales, for example the Alfvén waves, could be causing the deviations.

Some idea of the scale of the variations involved on the daily average timescale can be obtained from a closer examination of the $\phi_B - \phi_P$ and δ_B time series. A 90 day subset of the southern hemisphere high latitude time series of the $\phi_B - \phi_P$ and δ_B daily averages is plotted in Figure 11 (thin lines). For comparison we have over-plotted the predicted angles (heavy lines) calculated from the model of Zurbuchen *et al.* [1997] as described earlier. The predicted angles are dominated by the ~ 26 day solar rotation periodicity which, from equations (2)-(4), arises due to the rotation of the magnetic dipole axis

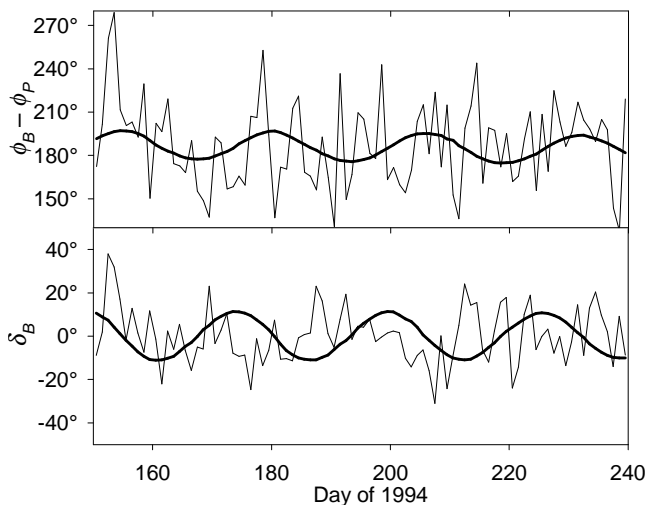


Figure 11. Plot showing the time series of $\phi_B - \phi_P$ and δ_B calculated from daily averaged magnetic field components (thin lines) for 90 days in 1994. The heavy lines show the model prediction of Zurbuchen *et al.* [1997].

about the rotation axis (the dipole axis being the symmetry axis of the over-expansion of the magnetic field lines within the polar coronal holes). The predicted amplitude is related to the differential rotation rate of the footpoints. We note that the amplitude of the general variability in the $\phi_B - \phi_P$ time series is larger than that of the dominant signal in the model while the variation in the δ_B time series is similar to the amplitude of the signal in the model. This suggests that any systematic variability in the magnetic field data produced by the physics in the *Fisk* model is going to be very hard to confirm even using the daily average timescale.

Although one might argue that the top panel of Figure 11 could be showing variability of $\phi_B - \phi_P$ around the sinusoidal prediction, a variability around a horizontal line at $\phi_B - \phi_P = 180^\circ$ looks just as believable. However, we chose the particular data segment shown in Figure 11 partly because the δ_B time series shows a suggestion of a quasi-periodic behaviour in a subset of the plot at about the same periodicity as in the model trace. This behaviour is apparent for a period of the order of 50 days (around days 160 to 210). It is the only time interval in either of the nine-solar-rotation data sets where such a periodicity stands out at all, hence why it did not show up in our nine-solar-rotation heliolongitude analysis. However, the signal in the data is clearly not in phase with the sinusoidal signal in the model. Although it may be fortuitous, we note that if we shift the model forward in time by ~ 7 days, equivalent to a change in ϕ_0 , there could be an approximate match between the data and the model during this time.

Evidence that signatures of the equatorial solar rotation period can be found in the magnetic field data even in regions where Ulysses was sampling only the uniform fast solar wind has been reported by *Denison et al.* [1999] using advanced spectral analysis techniques, although this periodicity did not show up in the autocorrelation analysis of the field data performed by *Zurbuchen et al.* [1997]. Thus at the very least we may have identified a region in the δ_B data where the signal reported by *Denison et al.* stands out more clearly.

In conclusion of this section, we suggest that our analysis using daily instead of hourly averaged data to calculate the field angles supports the hypothesis that the overwound most probable azimuth angle in the southern hemisphere and the double peaked distributions in the northern hemisphere are a result of the influence of the Alfvén waves on the angle distributions. However, based on the time series presented in Figure 11, our analysis does not rule out the possibility that the effects proposed by *Fisk* [1996] could be taking place.

Conclusions

In this paper we have presented distributions of the angles describing the direction of the heliospheric magnetic field throughout the different regions of the Ulysses first orbit of the Sun, during the declining and minimum phases of the solar cycle. To a first approximation both the azimuthal and meridional agree with the predictions of the simple Parker spiral model. However, two unexpected features noted were an overwound most probable azimuthal angle at high southern latitudes and a double peaked meridional angle distribution at high northern latitudes.

A search for heliolongitude dependence and a direct comparison with distributions deduced from published predictions

of the *Fisk* [1996] model show that the mechanisms of this model are unlikely to be the dominant cause of the above unexpected features. Together with an analysis using longer daily averaged data, the results point to the Alfvén waves present in the high latitude heliosphere being the most likely cause. Although we find no direct evidence that the effects described in the *Fisk* model are influencing our data, our results do not rule out that these effects could be occurring at an amplitude that is less than or similar to that of the general variability in the data. It is possible that the physical constraints on the model are time-variable to the extent that any signature does not remain coherent in the data for very long.

Since 1998 Ulysses has been continuing on its second orbit of the Sun at the same time as solar activity was rapidly rising towards solar maximum. Conditions at high latitudes are proving to be very different from the continuous fast solar wind found during the period described in this paper. The magnetic field direction during the present solar maximum is currently under study and will be the subject of a future publication.

Appendix A. Calculation of ϕ_B and δ_B

It may appear to be a straightforward process to calculate the azimuth angle ϕ_B and meridional angle δ_B describing the magnetic field direction given the three RTN magnetic field components (B_R , B_T , B_N). Using the components the angles may be obtained from

$$\tan \phi_B = B_T/B_R \quad \text{and} \quad \tan \delta_B = B_N/(B_R^2 + B_T^2)^{1/2} \quad (\text{A1})$$

However some care is required, particularly in calculating δ_B , resulting from the fact that we are using averaged data. Ulysses magnetic field data are typically sampled at a time resolution of 1 vector every 1 or 2 seconds depending on the spacecraft telemetry bit rate. By way of example, consider a situation where for the first half of an hour the magnetic field RTN components are (1, 1, 1) nT and for the second half of the hour they are (-1, 1, 1) nT. In both cases $\delta_B = 35.3^\circ$. But averaged over the hour the components become (0, 1, 1) nT which gives $\delta_B = 45^\circ$, a 10° overestimate using equations (A1). Similarly, the field magnitude $|\mathbf{B}|$ calculated from the hourly averaged components is underestimated at 1.41 nT compared to the true value of 1.73 nT.

Because of these known problems, the Ulysses averaged data sets also include the field magnitude $|\mathbf{B}|$ computed as an average of the individual full time resolution vector magnitudes during the averaging interval. This would be correctly recorded as an hourly average $|\mathbf{B}|$ of 1.73 nT in the above example. Thus the correct way to calculate the average field direction from the hourly averaged data set is by using the equations

$$\tan \phi_B = B_T/B_R \quad \text{and} \quad \sin \delta_B = B_N/|\mathbf{B}| \quad (\text{A2})$$

These equations applied to the hourly averaged vector (0, 1, 1) nT correctly give $\delta_B = 35.3^\circ$. When computing ϕ_B the signs of B_R and B_T are taken into account to give the correct value of ϕ_B in the range $0 - 360^\circ$. Both sets of equations correctly give the hourly average ϕ_B as 90° , half way between the two values of 45° and 135° obtained from the first and second halves of the hour.

These potential problems in calculating δ_B have been high-

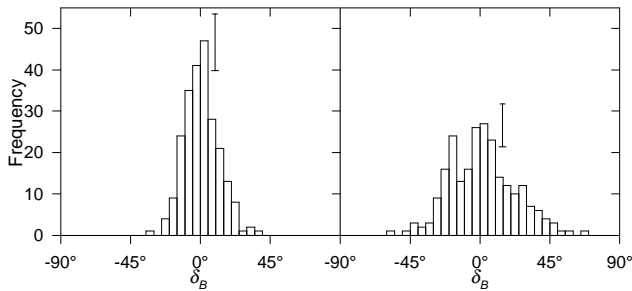


Figure 12. Comparison of the correct δ_B histogram (left) obtained using equation (A2) from daily averaged data with that (right) obtained using equation (A1).

lighted here as they become particularly acute for the daily averaged distributions presented in Figures 9 and 10. In these high latitude regions the presence of the Alfvén waves leads to many large direction changes in any one day period. Figure 12 compares the δ_B histogram from Figure 9 with that which would be obtained using equations (A1). The distribution on the right calculated using (A1) is significantly broader and more distorted than that on the left correctly obtained using (A2). The mean overestimate of δ_B using (A1) is 7.9° and the maximum is 39° .

Acknowledgements. Ulysses research at Imperial College is supported by the UK Particle Physics and Astronomy Research Council. Work at JPL was carried out under contract to NASA. We thank the Ulysses SWOOPS team (PI, D. J. McComas) for providing the solar wind speed data used in estimating ϕ_p .

References

- Balogh, A., T. J. Beek, R. J. Forsyth, P. C. Hedgecock, R. J. Marquedant, E. J. Smith, D. J. Southwood, and B. T. Tsurutani, The magnetic field investigation on the Ulysses mission: Instrumentation and preliminary scientific results, *Astron. Astrophys. Suppl. Ser.*, **92**, 221-236, 1992.
- Balogh, A., R. J. Forsyth, E. A. Lucek, T. S. Horbury, and E. J. Smith, Heliospheric magnetic field polarity inversions at high heliographic latitudes, *Geophys. Res. Lett.*, **26**, 631-634, 1999.
- Bame, S. J., D. J. McComas, B. L. Barraclough, J. L. Phillips, K. J. Sofaly, J. C. Chavez, B. E. Goldstein, and R. K. Sakurai, The Ulysses solar wind plasma experiment, *Astron. Astrophys. Suppl. Ser.*, **92**, 237-266, 1992.
- Bruno, R., and B. Bavassano, On the winding of the IMF spiral for slow and fast wind within the inner heliosphere, *Geophys. Res. Lett.*, **24**, 2267-2270, 1997.
- Burlaga, L. F., R. P. Lepping, K. W. Behannon, L. W. Klein, and F. M. Neubauer, Large-scale variations of the interplanetary magnetic field: Voyager 1 and 2 observations between 1-5 AU, *J. Geophys. Res.*, **87**, 4345-4353, 1982.
- Burlaga, L. F., and N. F. Ness, Large-scale distant heliospheric magnetic field: Voyager 1 and 2 observations from 1986 through 1989, *J. Geophys. Res.*, **98**, 17451-17460, 1993.
- Burlaga, L. F., and N. F. Ness, Global patterns of heliospheric magnetic field polarities and elevation angles: 1990 through 1995, *J. Geophys. Res.*, **102**, 19731-19742, 1997.
- Denison, D. G. T., A. T. Walden, A. Balogh, and R. J. Forsyth, Multitaper testing of spectral lines and the detection of the solar rotation frequency and its harmonics, *Appl. Statist.*, **48**, 427-439, 1999.
- Fisk, L. A., Motion of the footpoints of heliospheric magnetic field lines at the Sun: Implications for recurrent energetic particle events at high heliographic latitudes, *J. Geophys. Res.*, **101**, 15547-15553, 1996.
- Forsyth, R. J., A. Balogh, E. J. Smith, N. Murphy and D. J. McComas, The underlying magnetic field direction in Ulysses observations of the southern polar heliosphere, *Geophys. Res. Lett.*, **22**, 3321-3324, 1995.
- Forsyth, R. J., A. Balogh, E. J. Smith, G. Erdős and D. J. McComas, The underlying Parker spiral structure in the Ulysses magnetic field observations, 1990-1994, *J. Geophys. Res.*, **101**, 395-403, 1996a.
- Forsyth, R. J., A. Balogh, T. S. Horbury, G. Erdős, E. J. Smith and M. E. Burton, The heliospheric magnetic field at solar minimum: Ulysses observations from pole to pole, *Astron. Astrophys.*, **316**, 287-295, 1996b.
- Forsyth, R. J., A. Balogh, E. J. Smith, and J. T. Gosling, Ulysses observations of the northward extension of the heliospheric current sheet, *Geophys. Res. Lett.*, **24**, 3101-3104, 1997.
- Horbury T. S., and Balogh, A., Evolution of magnetic field fluctuations in high speed solar wind streams: Ulysses and Helios observations, *J. Geophys. Res.*, in press, 2001.
- Marsden, R. G., E. J. Smith, J. F. Cooper and C. Tranquille, Ulysses at high heliographic latitudes: an introduction, *Astron. Astrophys.*, **316**, 279-286, 1996.
- McComas, D. J., B. L. Barraclough, H. O. Funsten, J. T. Gosling, E. Santiago-Muñoz, R. M. Skoug, B. E. Goldstein, M. Neugebauer, P. Riley, and A. Balogh, Solar wind observations over Ulysses' first full polar orbit, *J. Geophys. Res.*, **105**, 10419-10433, 2000.
- Phillips, J. L., A. Balogh, S. J. Bame, B. E. Goldstein, J. T. Gosling, J. T. Hoeksema, D. J. McComas, M. Neugebauer, N. R. Sheeley, Jr., and Y.-M. Wang, Ulysses at 50° : Constant immersion in the high-speed solar wind, *Geophys. Res. Lett.*, **21**, 1105-1108, 1994.
- Ness, N. F., and J. M. Wilcox, Solar origin of the interplanetary magnetic field, *Phys. Rev. Lett.*, **13**, 461-464, 1964.
- Parker, E. N., Dynamics of the interplanetary gas and magnetic fields, *Astrophys. J.*, **128**, 664-676, 1958.
- Roelof, E. C., G. M. Simnett, and S. J. Tappin, The regular structure of shock-accelerated ~ 40 -100 keV electrons in the high latitude heliosphere, *Astron. Astrophys.*, **316**, 481-486, 1996.
- Sanderson, T. R., V. Bothmer, R. G. Marsden, K. J. Trattner, K.-P. Wenzel, A. Balogh, R. J. Forsyth, and B. E. Goldstein, The Ulysses south polar pass: Energetic ion observations, *Geophys. Res. Lett.*, **22**, 3357-3360, 1995.
- Smith, C. W., and J. W. Bieber, Multiple spacecraft survey of the north-south asymmetry of the interplanetary magnetic field, *J. Geophys. Res.*, **98**, 9401-9415, 1993.
- Smith, E. J., Solar wind magnetic fields, in *Cosmic winds and the heliosphere*, edited by J. R. Jokipii, C. P. Sonett, and M. S. Giampapa, pp. 425-457, University of Arizona Press, Tucson, 1997.
- Smith, E. J., A. Balogh, M. Neugebauer and D. J. McComas, Ulysses observations of Alfvén waves in the southern and northern solar hemispheres, *Geophys. Res. Lett.*, **22**, 3381-3384, 1995.
- Smith, E. J., A. Balogh, M. Burton, R. J. Forsyth, and R. P. Lepping, Radial and azimuthal components of the heliospheric magnetic field: Ulysses observations, *Adv. Space Res.*, **20**, 47-53, 1997a.
- Smith, E. J., M. Neugebauer, B. T. Tsurutani, A. Balogh, R. J. Forsyth, and D. J. McComas, Properties of hydromagnetic waves in the polar caps: Ulysses, *Adv. Space Res.*, **20**, 55-63, 1997b.
- Smith, E. J., A. Balogh, R. J. Forsyth, B. T. Tsurutani, and R. P. Lepping, Recent observations of the heliospheric magnetic field at Ulysses: Return to low latitude, *Adv. Space Res.*, **26**, 823-832, 2000.
- Thomas, B. T., and E. J. Smith, The Parker spiral configuration of the interplanetary magnetic field between 1 and 8.5 AU, *J. Geophys. Res.*, **85**, 6861-6867, 1980.
- Zurbuchen, T. H., N. A. Schwadron, L. A. Fisk, Direct observational evidence for a heliospheric magnetic field with large excursions in latitude, *J. Geophys. Res.*, **102**, 24175-24181, 1997.